

Effects of magnesium chloride-based multicomponent salts on atmospheric corrosion of aluminum alloy 2024

Bin-bin WANG, Zhen-yao WANG, Wei HAN, Chuan WANG, Wei KE

State Key Laboratory for Corrosion and Protection, Institute of Metal Research,
Chinese Academy of Sciences, Shenyang 110016, China

Received 28 March 2012; accepted 25 May 2012

Abstract: Atmospheric corrosion of aluminum alloy 2024 (AA2024) with salt lake water was simulated through a laboratory-accelerated test of cyclic wet-dry and electrochemical techniques. Effects of the soluble magnesium salt contained in the salt water were investigated by scanning electron microscope (SEM), transmission electron microscope (TEM), energy dispersive spectrometer (EDS), electron probe micro analyzer (EPMA), X-ray diffraction (XRD), infrared transmission spectroscopy (IR), and atmospheric corrosion monitor (ACM). The results showed that, with the deposition, atmospheric corrosion of AA2024 could occur when the relative humidity (RH) was lower than 30%. A main crystalline component of corrosion products, layered double hydroxides (LDH), $[\text{Mg}_{1-x}\text{Al}_x(\text{OH})_2]^{x+} \text{Cl}_x^- \cdot m\text{H}_2\text{O}$ (LDH-Cl), was determined, which meant that magnesium ion played an important role in the corrosion process. It not only facilitated the corrosion as a result of deliquescence, but also was involved in the corrosion process as a reactant.

Key words: aluminum alloy 2024; atmospheric corrosion; magnesium chloride; relative humidity; corrosion products

1 Introduction

Aluminum and its alloys have been extensively used in the fields of transport, building, aircraft and aerospace. In these fields, atmospheric corrosion will occur in various forms, which depends on the environmental conditions. In unpolluted atmosphere, aluminum and its alloys have good corrosion resistance. While, in polluted atmosphere, they will suffer severe corrosion, especially in marine environment with the deposition of chloride-aerosols which can cause severe damage to passive film formed on metal surface [1–5]. Various corrosion behaviors of aluminum and its alloys in marine atmosphere are always attributed to the high relative humidity and deposition of sea-salt particles [2].

Salt lakes are widely distributed in Western China. As well as the high chlorides deposition is concerned, these regions belong to an arid-climate region with small precipitation and large evaporation, and the annual relative humidity varies from 30% to 50%, or lower [6], which are different from desert atmosphere and marine atmosphere. With the deepening of the western

development of China, the corrosiveness of arid and salt-rich atmosphere for common metals in basic construction has drawn enormous attention. It was reported that in arid and salt-rich atmosphere, aluminum and its alloys (like AA2024) suffered more severe corrosion than in marine environment and acid rain environment [7–10]. It is well known that due to the moisture absorption of polluted deposition like chlorides, it will facilitate the atmospheric corrosion in lower relative humidity [11,12]. Therefore, the serious corrosion behaviors of aluminum in arid and salt-rich atmosphere were attributed to the high salts deposited simply. However, in marine atmosphere with the similar deposition amount, the corrosion of aluminum was less serious. On the contrary, the corrosion rate of carbon steels in the arid and salt-rich atmosphere was much lower than that in marine atmosphere [7,13,14].

It was found that these regions were abundant in magnesium salt which was different from seawater [6,12]. However, investigations of the effects of cations like Mg^{2+} on the corrosion of metals were scarce. Furthermore, the laboratory studies performed in controlled environments presented discrepancy results

about the effects of different cations, and the role of magnesium ions in the forming of corrosion products was not reported [12,15,16].

Considering the effects of chloride deposits on different metals and the previous studies, it is believed that some other factors influence the corrosion behavior of aluminum induced by the deposition in arid and salt-rich atmosphere. Firstly, in outdoor environments, salt particles deposited on the metal surface exist as aerosols which are multicomponent and mixed. The deliquescence and efflorescence behaviors of multicomponent mixed-salts are more complicated than those of single-component salt, which will significantly influence the time of wetness (TOW) on metal surface in arid atmospheric environment [17]. Secondly, when compared with the chemical synthesis of magnesium–aluminum layered double hydroxides (LDHs) according to a coprecipitation reaction, it was found that with magnesium chloride deposition, reaction conditions in atmospheric corrosion process of aluminum and aluminum alloys were similar to those in the coprecipitation reaction [18]. Thus, it is reasonable to postulate that magnesium salt plays an important role in the process of corrosion product formed.

In this work, the effects of magnesium chloride (MgCl_2)-based multicomponent mixed-salts on the TOW of atmospheric corrosion of AA2024 in low relative humidity environment and the role of magnesium ions in the process of corrosion product forming were investigated through galvanic current measurement and analysis of corrosion products, respectively.

2 Experimental

2.1 Materials preparation

Commercial AA2024-T3 plates were used for the test and their chemical compositions are given in Table 1. The sizes of samples were 100 mm×50 mm×0.9 mm. The alloy material was clad with a layer of aluminum for increasing the corrosion resistance. Thus, the layer was removed using 5% NaOH solution at 75 °C. The thickness of the samples without cladding was 0.7 mm. Prior to test, all the samples were degreased with acetone, rinsed using ethanol, and weighed (exactness 0.1 mg) by analytic balance after drying.

Table 1 Chemical compositions of AA2024-T3 (mass fraction, %)

Fe	Si	Cu	Mn	Zn	Mg	Al
0.50	0.50	4.18	0.30	0.30	1.30–1.80	Bal.

A copper–AA2024 coupled electrode with comb-like arrangement was used in galvanic current

measurement. The schematic diagram of the monitoring electrode is shown in Fig. 1. Each metal slices of the electrode was 20 mm×5 mm×1.5 mm, and the insulating spacing between each slice was 300 μm . The electrode was mechanically ground down to 1000 grit SiC paper.

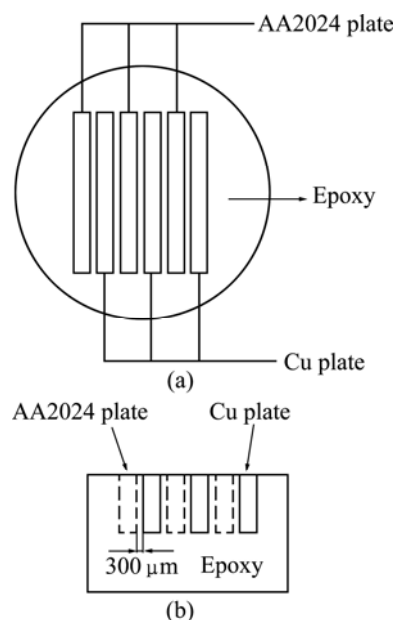


Fig. 1 Schematic of monitoring electrode: (a) Top view; (b) Transverse cross-sectional view

2.2 Simulated tests

2.2.1 Galvanic current measurement

In order to investigate the effect of salt-deposition on the time of wetness (TOW) of atmospheric corrosion of AA2024, the galvanic current of the electrode with MgCl_2 -based multicomponent mixed-salts deposited was detected in different relative humidity (RH) environments varying from 10% to 80% using an atmospheric corrosion monitor. A WDB-5A aerosol sprayer filled with MgCl_2 -based salt lake water was used to deposit micro-droplets on the electrode surface. The compositions of salt lake water are listed in Table 2. Then, the electrodes were put into a vacuum desiccator. After drying, salt particles were deposited on the electrodes with different amount (5 mg/cm^2 and 0.5 mg/cm^2). The relative humidity in the simulated environment was achieved by a series of different saturated salt solutions placed in a closed chamber. RH was monitored using a humidity meter with error of $\pm 1\%$. And the temperature was maintained at (20 ± 0.5) °C. Putting the electrode with deposition into environment chamber from lower RH to higher RH respectively, the galvanic current was recorded when the current was stable. After each record as well as the moisture absorption of salt particles did not change at a certain RH, the electrode was placed in an environment with the RH much lower than the deliquescence relative humidity

(DRH) of the salt particles (22% RH and 11% RH). Then, the galvanic current was recorded every 10 s during the drying process. The duration of each test varied from 2 h to 5 h in order to obtain the stable current and to maintain the uniformity of the electrode surface. After each drying process, the salt particles were redeposited according to the steps described above.

Table 2 Compositions of salt lake water (mass fraction, %)

K ⁺	Na ⁺	Ca ²⁺	Mg ²⁺	Cl ⁻	SO ₄ ²⁻
1.4	1.2	0.21	6.7	22.5	0.49

2.2.2 Laboratory-accelerated test of cyclic wet-dry

The accelerated corrosion tests were performed using a DW-UD-3 type Combined Cyclic Corrosion Test Instrument with salt lake water diluted 10 times. The test parameters are listed in Table 3. The test was performed for 240 h, and the specimens were withdrawn for analyzing every 48 h.

Table 3 Parameters of immersion-dry-wet cycles acceleration experiments

State	Temperature/°C	Time/min
Immersion	40	1
Dry	40	6
Wet	45	2

2.3 Analysis of corrosion products

For surface observation by scanning electron microscopy (SEM, XL30FEG), the samples were cut into the sizes of 20 mm×20 mm, and the elemental composition was determined by energy dispersive X-ray diffraction (EDX).

Cross sections of the corroded samples were mechanically ground down to 1500 grit SiC paper, and polished with 1.5 μm diamond pastes. After that, the samples were used for studying the distribution of some important elements in the cross-section by a Shimadzu Model EPMA-1610 electron probe micro analyzer at 15 kV acceleration voltage.

The corrosion products were scraped off using a razor blade and characterised by means of X-ray diffraction (XRD). A step-scanning X-ray diffractometer was used, with copper K_α radiation, in the scanning range of 10°–90°. For infrared transmission spectroscopy (IRS) analysis, 5 mg of the corrosion product was mixed with 50 mg pure potassium bromide and the mixture was pressed into a transparent circular flake. A Magna-IR 560 infrared spectrophotometer was used to determine the IR spectra in the range of 400–4000 cm⁻¹ with the accuracy of 8 cm⁻¹.

Furthermore, the microstructure of the corrosion products and the main elements in the corrosion products

were studied. First, the corrosion product powders were ultrasonically dispersed to suspend in ethanol, then several drops of suspension were dipped on a carbon film supported on a copper grid with the size of $d3\text{ mm}\times 20\text{ nm}$. After they were dried in a vacuum desiccator, the samples were observed by FEI Tecnai g20 transmission electron microscope (TEM).

3 Results and discussion

3.1 Galvanic current measurement

3.1.1 Galvanic current of electrode in different relative humidity

The trends of galvanic current of electrode with deposition in different relative humidity are shown in Fig. 2. The galvanic current showed an increasing trend as the relative humidity increased. In the case of salt deposition of 0.5 mg/cm² (Fig. 2(a)), the current was detected at 31.4% RH. As the RH reached the DRH of magnesium chloride hexahydrate (DRH of magnesium chloride hexahydrate in the test conditions was 34% RH), the current grew sharply, whereas the current decreased slightly when the RH increased a small value above the DRH. When further increasing the RH, the current was raised obviously. Similar trend was observed in the

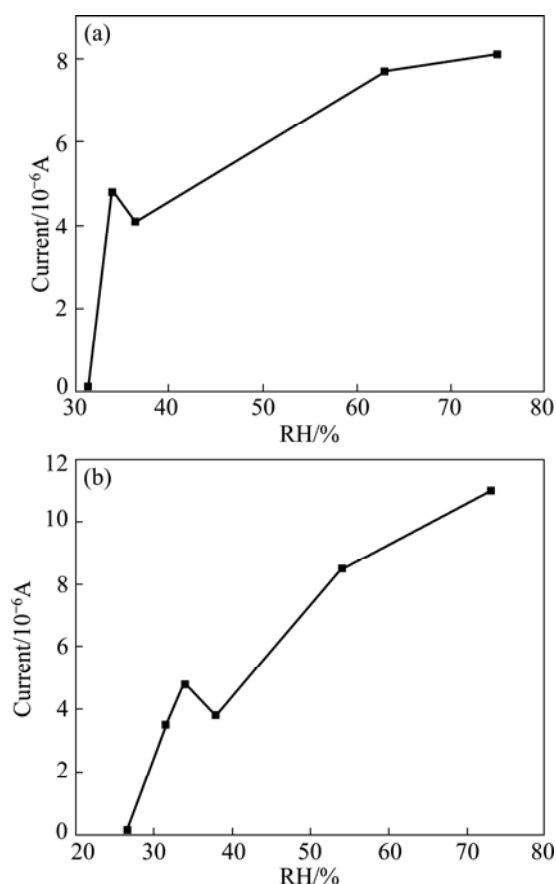


Fig. 2 Galvanic current of electrode covered with salts vs relative humidity: (a) Salt deposition of 0.5 mg/cm²; (b) Salt deposition of 5 mg/cm²

case of salt deposition of 5 mg/cm^2 (Fig. 2(b)), whereas the current was detected at lower RH (26.5% RH). And at a certain RH, the more the salt particles deposited, the higher the current was.

The corrosion rate of metal in neutral electrolyte layer was determined by both cathodic oxygen reduction and anodic process. Below the DRH of salt particles, due to the extreme thin film formed on the metal, the diffusion of the oxygen was quite easy, thus the corrosion process was probably controlled by the anodic process. Meanwhile, the electrolyte did not cover the entire metal surface. Therefore, the current increased at a low level as the RH rose. As the DRH was reached, salt particles deliquesced to thin electrolyte and covered the entire surface. Both the diffusion of oxygen and metal ions was relatively easy, which resulted in the sharp increasing of current. Further increasing the RH in a small range, the thickness of the electrolyte increased slightly as well as the diffusion of metal ions. However, the cathodic oxygen reduction process could slow down if the thickness of electrolyte reached a certain level and was independent of the thickness of the electrolyte when RH achieved a particular value [19]. Thus, there was a decline of the current when the RH exceeded the DRH slightly. As the RH kept growing, the anodic process became more facile. And, instead of the anodic process, cathodic oxygen reduction was the rate-determining step which accounted for the increasing trend of current after the RH exceeded the DRH. Due to the localized corrosion of AA2024 in test conditions, the galvanic current showed discrete in parallel tests as well as the RH at which the current decreased. However, similar trend was observed in each parallel test.

3.1.2 Galvanic current of electrode in drying process

The trend of galvanic current of electrode with deposition in drying process is shown in Figs. 3 and 4. In the case of salt deposition of 5 mg/cm^2 (Fig. 3), when the electrode with deposition absorbed water was in higher RH environment than the DRH, the current declined sharply in 1 h and then tended to remain stable with a relatively higher current until the test was over; when the RH was equal to the DRH, similar trend with lower current and shorter duration was observed (Fig. 3(a)). Whereas, if the RH was lower than the DRH, the current decreased quickly and disappeared in a short time, as shown in Figs. 3(b) and (c). And the platform region presented in Fig. 3(c) could be probably attributed to the pitting corrosion occurring during the drying process which kept the current unchanged in a short time. In the case of 0.5 mg/cm^2 , the trend was similar to that in the case of 5 mg/cm^2 , as shown in Fig. 4.

From the results presented above, it can be seen that

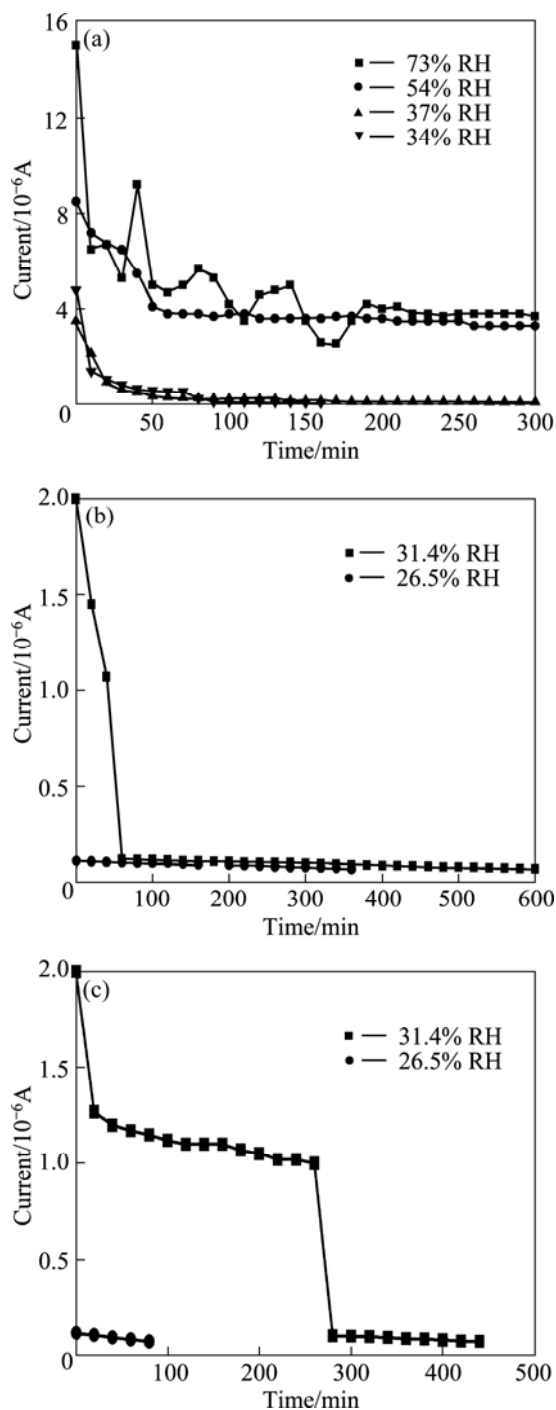


Fig. 3 Change of galvanic current in drying process after electrode absorbing water in different RH conditions (salt deposition of 5 mg/cm^2): (a) Absorbing water at higher RH and being dried at 11% RH; (b) Absorbing water at lower RH and being dried at 22% RH; (c) Absorbing water at lower RH and being dried at 11% RH

corrosion occurred in much lower RH environment due to the existence of soluble magnesium salt with lower DRH. However, it is generally accepted that in low RH environment, if the RH is lower than the DRH of the deposition, the corrosion will not occur or can be neglected [20,21]. In fact, the salt particles deposited on

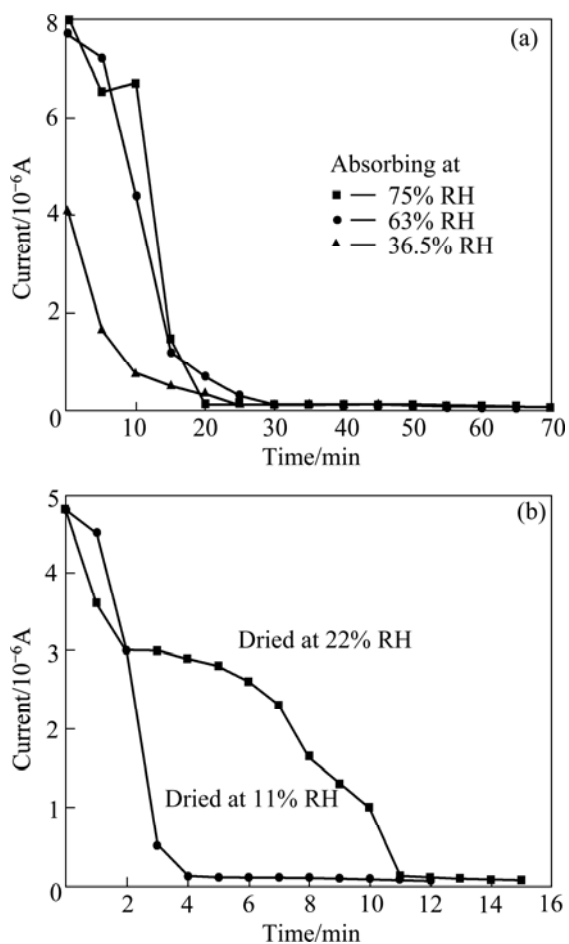


Fig. 4 Change of galvanic current in drying process after electrode absorbing water in different RH conditions (salt deposition of 0.5 mg/cm^2): (a) Absorbing water at higher RH and being dried at 11% RH; (b) Absorbing water at lower RH (31.4% RH) and being dried at 11% RH, 22% RH respectively

the metal surface were multicomponent and existed in the internal-mixed form. For multicomponent salt particles, the deliquescence and efflorescence behaviors are more complicated than those of the single-component salt particles. The DRH of multicomponent salt particles is lower than that of individual components. And the DRH of the mixture does not have a certain value, but is a function of the mixed salts. The minimum DRH of multicomponent salt particles is called mutual deliquescence relative humidity (MDRH). At MDRH the aqueous solution is saturated with respect to each solute [17]. For instance, as the RH decreases over an aqueous particle with multicomponent, particles dried from supersaturated solution are composed of a pure salt core that is the least soluble component, surrounded by a mixed salt coating. The core composition is only determined by the original aerosol composition, while the coating is identical with the eutonic composition and is independent of the original aerosol composition [22].

Conversely, as the RH increases, the outermost layer of the coating is first dissolved in the absorbed water when the RH reaches the MDRH. When further increasing the RH, more water will be absorbed into the particles, which results in part of the salt solid core dissolved. Then, the salt solid core will be completely dissolved into the solution at a certain RH, the value of which is a function of the overall composition of the mixed salt particle [23]. Furthermore, even in the case of single-component salt particles deposition, during drying process, the droplet passes the deliquescence point without phase change and becomes highly supersaturated as a metastable droplet. Finally, crystallization takes place until a certain RH is reached which is much lower than the DRH of the salt [24]. For example, the efflorescence relative humidity (ERH) of sodium chloride is about 45%, which is much lower than the DRH (about 75%) [25]. However, in a bulk solution, crystallization always occurs not far beyond the saturation point.

Therefore, the relatively higher current at the RH that was lower than the DRH of magnesium chloride hexahydrate could be probably attributed to the deliquescence of the outermost layer of the eutonic composition of the particles. And, in the case of salt deposition of 0.5 mg/cm^2 , the galvanic current could be detected at a slightly higher RH (31.4%) than that in the case of 5 mg/cm^2 (26.5%). The reason for the discrepancy may be ascribed to the uncontinuous electrolyte film formed on the electrode surface due to the less deposition and the wider insulating spacing between each slice of the electrode.

Then, considering the abundant magnesium chloride and little calcium chloride contained in the salt lake water, which both have lower DRH, electrolyte in which corrosion occurred can be formed under RH lower than 30%, as a result of the deliquescence of particles deposited on the metal surface. It can be inferred that before the protective corrosion product layers form on the metal surface, TOW of the samples surface is much longer than the value calculated from the DRH of magnesium chloride which could partially account for the serious atmospheric corrosion of aluminum and aluminum alloys in arid and salt-rich atmosphere.

In addition, at the DRH of MgCl_2 -based multicomponent mixed-salts and MgCl_2 respectively, the chloride concentration in multicomponent solution droplet is higher than that in MgCl_2 solution droplet. And both of them are much higher than that in NaCl solution droplet, resulting in more serious damage to metal surface like aluminum and stainless steel [26,27]. However, it is the effect of Cl^- on deterioration of passive film formed on metal surface that will not be discussed in this work.

3.2 Observation and analysis of corrosion products and morphology

3.2.1 Analysis of corrosion morphology

The surface of samples was covered with pits and white corrosion products. SEM morphology with different magnifications and EDX spectrum of corrosion products of the samples tested for 240 h are shown in Fig. 5. It is apparent that there were many microcracks around the pits, and sheet corrosion products were formed in the region beside the pits. The chemical compositions of the marked site were determined by EDX. The EDX spectrum revealed the presence of aluminum, oxygen, magnesium, chlorine elements in the corrosion products. The last two elements were obviously from the salts that deposited on the samples. Therefore, it was reasonable to postulate that magnesium ions played an important role in the corrosion process. The cross-sectional morphology and distributions of chlorine, magnesium and oxygen elements in the corrosion products formed on the sample tested for 240 h are presented in Fig. 6. It could be seen that chlorine and magnesium elements were distributed throughout the corrosion products homogeneously, as a further proof that magnesium ions had taken part in the corrosion process.

3.2.2 Analysis of corrosion products

XRD patterns of the corrosion products formed on the samples tested for different periods are shown in Fig. 7. In combination with the elements in the corrosion products and the prior results, an inorganic layered material, $[\text{Mg}_{1-x}\text{Al}_x(\text{OH})_2]^{x+} \text{Cl}_x^- \cdot n\text{H}_2\text{O}$ (LDH-Cl) as corrosion product, was determined. Meanwhile, no bayerite and alumina that are two common corrosion products of aluminum and aluminum alloys in sodium chloride solution were determined.

IR spectra of the corrosion products formed on the samples tested for different periods are shown in Fig. 8. With lengthening of the test time, there was an obvious increase in crystallinity. According to the previous report [28], the results obtained from the IR spectra were in agreement with those obtained by XRD analysis.

Figure 9 displays the TEM photograph of the corrosion product and the chemical compositions of the marked sites. The corrosion products were mainly sheet particles of nano-crystalline, among which there were some amorphous particles that could not be determined. From the results of EDX spectrum, elements contained in the corrosion products were consistent with the EDX results shown above, but there was a slight difference in content depending on different sites, which meant that the corrosion products were nonstoichiometric compounds but a series of compounds with the similar

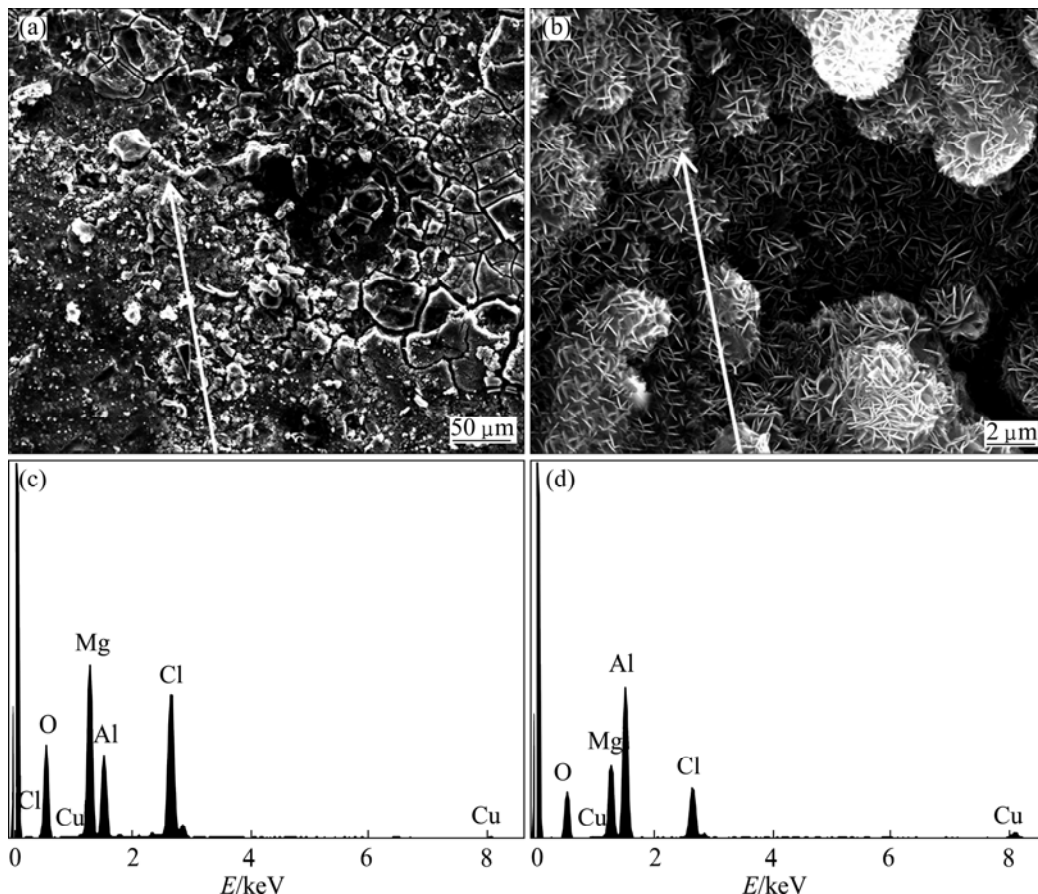


Fig. 5 SEM morphologies with different magnifications and EDX spectra of corrosion products of samples tested for 240 h

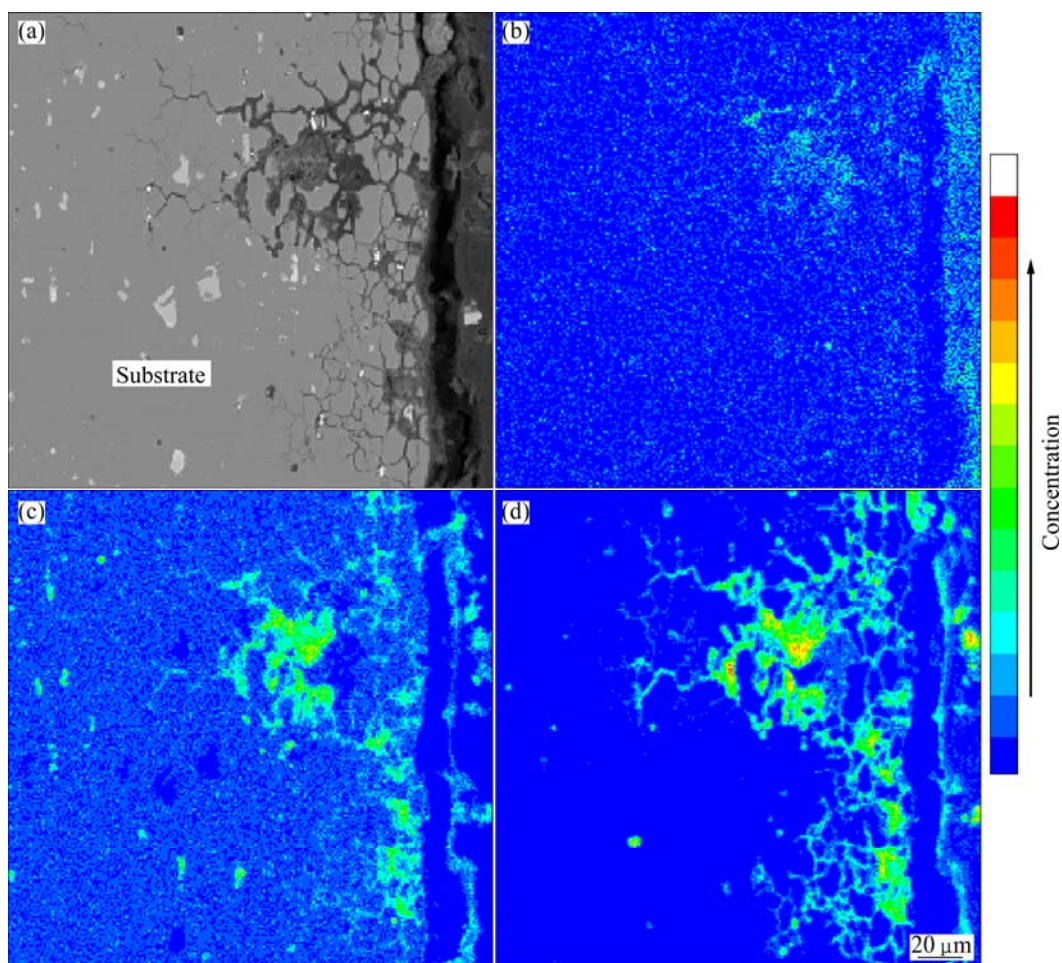


Fig. 6 Cross-sectional morphology (a) and distribution of Cl (b), Mg (c) and O (d) in corrosion products formed on sample tested for 240 h

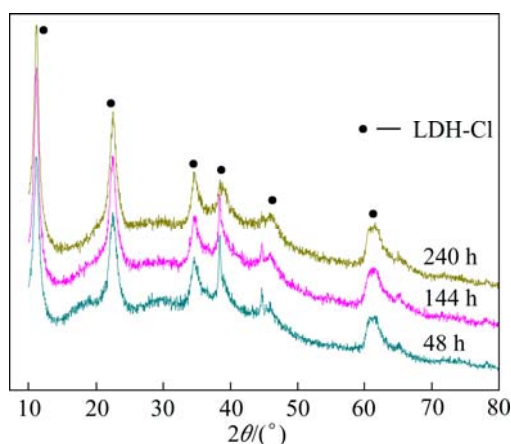


Fig. 7 XRD patterns of corrosion products formed on samples with different test periods

crystal structure called layered double hydroxides (LDH). This result was also consistent with that obtained in chemical synthesis of LDH [28]. On the other hand, it was difficult to form a pure corrosion product due to the changed environment of electrolyte formed on the metal surface under atmosphere conditions.

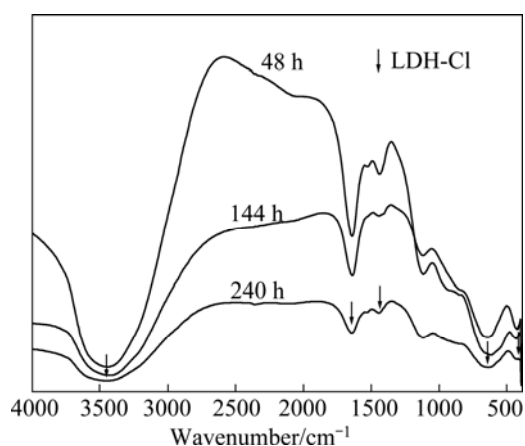


Fig. 8 IR spectra of corrosion products formed on samples with different test periods

LDHs have the general formula of $[M_{1-x}^{2+}M_x^{3+}(\text{OH})_2]^x(A^{n-})_{x/n} \cdot m\text{H}_2\text{O}$, where M^{2+} and M^{3+} are divalent and trivalent metal ions such as Mg^{2+} and Al^{3+} , respectively, and A^{n-} is n -valent anion [18]. It is impossible to form LDH with univalent metal ions like Na^+ and K^+ in the corrosion process of aluminum and its

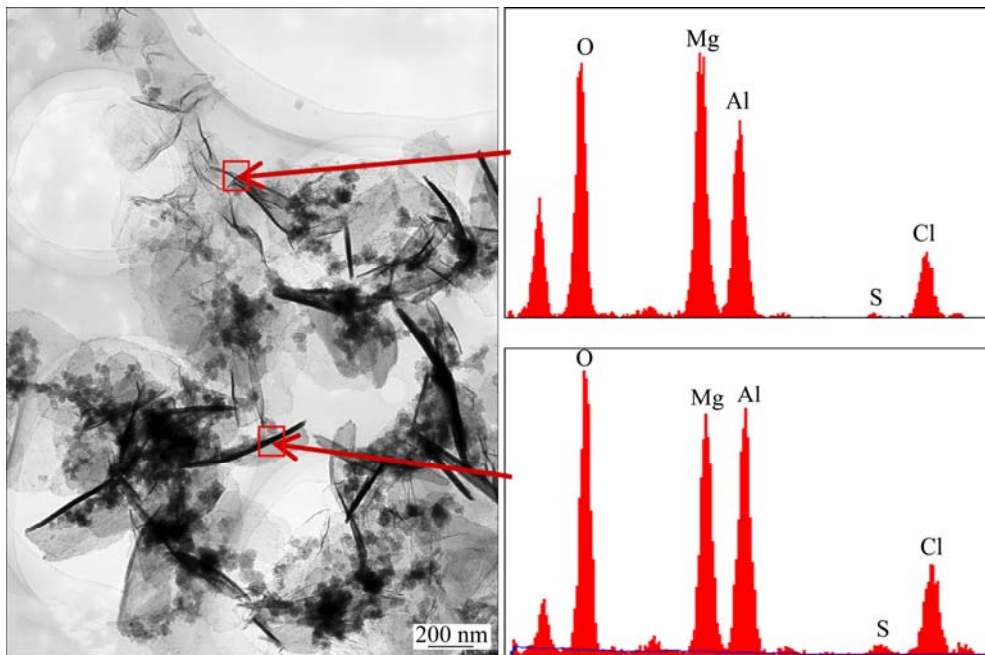


Fig. 9 TEM morphology and EDX spectra of corrosion products of sample tested for 240 h

alloys. Heretofore, reports on the corrosion products of LDH formed in the corrosion process of aluminum in electrolyte containing divalent metal ions like Mg^{2+} are scarce. According to a coprecipitation reaction, LDH can be synthesized by a mixture solution of magnesium chloride and aluminium chloride at pH 8–10 [18,28]. The pH and certain degree of supersaturation of the solution are two key-factors in the synthesis, which can be met in the corrosion process of AA2024. First, in the test environment, bayerite formed due to the corrosion of AA2024. At the same time, along with pH value increasing of cathodic areas where oxygen reduction took place [29–32], brucite precipitated. Then, after some complicated steps between bayerite and brucite, LDH-Cl formed [28]. As the secondary corrosion products with small amount, LDHs were found in the corrosion products of steel and zinc–aluminum alloys [33–35], while in this case, LDH was formed as the main corrosion products.

Based on the formation mechanism of LDH, lack of alumina and bayerite in corrosion products could be attributed to the transformation of corrosion products from alumina and bayerite to LDH. Due to the transformation of primary corrosion products, the formation of LDH led to the further corrosion of substrate from the perspective of chemical equilibrium, which was another reason for the higher corrosivity of magnesium chloride than that of sodium chloride as reported before.

As described above, it was clear that magnesium salt played an important role in the corrosion of AA2024

which was different from that induced by sodium salt. On one hand, the TOW on metal surface was extended due to the complicated deliquescence and efflorescence behaviors of $MgCl_2$ -based multicomponent salts in low relative humidity. On the other hand, the formation of LDH-Cl which led to the disappearance of bayerite and alumina confirmed that magnesium ions took part in the corrosion process of AA2024 as a reactant.

4 Conclusions

1) Due to the deliquescence of $MgCl_2$ -based multicomponent salt particles, corrosion occurred at the relative humidity that was much lower than the DRH of magnesium chloride hexahydrate.

2) In the drying process of electrode absorbed water in high relative humidity environment, the duration of current was much longer than anticipation, which extended the time of wetness.

3) $[Mg_{1-x}Al_x(OH)_2]^{x+}Cl_x^- \cdot mH_2O$ was determined as the main corrosion products, which meant that magnesium element was involved in the corrosion process as a reactant.

References

- [1] DEAN S W, ANTHONY W H. Atmospheric corrosion of wrought aluminum alloys during a ten-year period [C]//DEAN S W, LEE T S. Degradation of Metals in the Atmosphere. Philadelphia: American Society of Testing and Materials, 1988: 191–205.
- [2] CAO Chu-nan. Material natural environmental corrosion of China [M]. Beijing: Chemical Industry Press, 2005: 108–124. (in Chinese)

- [3] VERA R, DELGADO D, ROSALES B M. Effect of atmospheric pollutants on the corrosion of high power electrical conductors: Part 1. Aluminum and AA6201 alloy [J]. *Corrosion Science*, 2006, 48: 2882–2900.
- [4] da la FUENTE D, OTERO-HUERTA E, MORCILLO M. Studies of long-term weathering of aluminum in the atmosphere [J]. *Corrosion Science*, 2007, 49: 3134–3148.
- [5] SUN Shuang-qing, ZHENG Qi-fei, LI De-fu, WEN Jun-guo. Long-term atmospheric corrosion behavior of aluminum alloys 2024 and 7075 in urban, coastal and industrial environments [J]. *Corrosion Science*, 2009, 51: 719–727.
- [6] ZHENG Xi-yu, ZHANG Ming-gang, XU Chang, LI Bing-xiao. Records of Chinese salt lakes [M]. Beijing: Science Press, 2002: 14–43. (in Chinese)
- [7] XIAO Yi-de, WANG Guang-yong, LI Xiao-gang, LIN An, ZHANG San-ping, QIN Xiao-zhou, WANG Zhen-yao, LIANG Cai-feng, ZHENG Qi-fei, MAO Hai-rong. Corrosion behavior of atmospheric environment and corrosion feature of materials in our western area [J]. *Journal of Chinese Society for Corrosion and Protection*, 2003, 23(4): 248–255. (in Chinese)
- [8] ZHENG Qi-fei, SUN Shuang-qing, WEN Jun-guo, LI De-fu. Atmospheric corrosion behaviors of aluminum and aluminum alloys in desert atmosphere of southern Xinjiang Province [J]. *The Chinese Journal of Nonferrous Metals*, 2009, 19(2): 353–359. (in Chinese)
- [9] WANG Zhen-yao, LI Qiao-xia, WANG Chuan, HAN Wei, YU Guo-cai. Corrosion behaviours of Al alloy LC4 in Geremu salt lake atmosphere [J]. *The Chinese Journal of Nonferrous Metals*, 2007, 17(1): 24–29. (in Chinese)
- [10] WANG Bin-bin, WANG Zhen-yao, HAN Wei, KE Wei. Atmospheric corrosion of aluminium alloy 2024-T3 exposed to salt lake environment in western China [J]. *Corrosion Science*, 2012, 59: 63–70.
- [11] WALL F D, MARTINEZ M A, MISSERT N A, COPELAND R G, KILGO A C. Characterizing corrosion behavior under atmospheric conditions using electrochemical techniques [J]. *Corrosion Science*, 2005, 47: 17–32.
- [12] SUN Shuang-qing, ZHENG Qi-fei, WEN Jun-guo, LI De-fu. Atmospheric corrosion of aluminum in the northern Taklamakan Desert environment [J]. *Materials and Corrosion*, 2010, 61(10): 852–859.
- [13] LI Qiao-xia, WANG Zhen-yao, HAN Wei, HAN En-hou. Characterization of the rust formed on weathering steel exposed to Qinghai Salt Lake atmosphere [J]. *Corrosion Science*, 2008, 50: 365–371.
- [14] LI Qiao-xia, WANG Zhen-yao, HAN Wei, HAN En-hou. Characterization of the corrosion products formed on carbon steel after exposed to the open atmosphere in Qinghai Salt Lake [J]. *Corrosion*, 2007, 63: 640–647.
- [15] BLÜCHER D B, SVENSSON J E, JOHANSSON L G. The influence of CO₂, AlCl₃·6H₂O, MgCl₂·6H₂O, Na₂SO₄ and NaCl on the atmospheric corrosion of aluminum [J]. *Corrosion Science*, 2006, 48: 1848–1866.
- [16] PROSEK T, THIERRY D, TAXÉN C, MAIXNER J. Effect of cations on corrosion of zinc and carbon steel covered with chloride deposits under atmospheric conditions [J]. *Corrosion Science*, 2007, 49: 2676–2693.
- [17] WEXLER A S, SEINFELD J H. Second-generation inorganic aerosol model [J]. *Atmospheric Environment A*, 1991, 25: 2731–2748.
- [18] CONSTANTINO V R L, PINNAVAIA T J. Basic properties of Mg_{1-x}Al_x²⁺, layered double hydroxides intercalated by carbonate, hydroxide, chloride, and sulfate anions [J]. *Inorganic Chemistry*, 1995, 34(4): 883–892.
- [19] CHENG Y L, ZHANG Z, CAO F H, LI J F, ZHANG J Q, WANG J M, CAO C N. A study of the corrosion of aluminum alloy 2024-T3 under thin electrolyte layers [J]. *Corrosion Science*, 2004, 46: 1649–1667.
- [20] ISO 9223. Corrosion of metals and alloys — Corrosivity of atmospheres—Classification [S]. 1992.
- [21] LI Chun-ling, MA Yuan-tai, LI Ying, WANG Fu-hui. EIS monitoring study of atmospheric corrosion under variable relative humidity [J]. *Corrosion Science*, 2010, 52: 3677–3686.
- [22] GE Z Z, WEXLER A S, JOHNSTON M V. Multicomponent aerosol crystallization [J]. *Journal of Colloid and Interface Science*, 1996, 183: 68–77.
- [23] GE Z Z, WEXLER A S, JOHNSTON M V. Deliquescence behavior of multicomponent aerosols [J]. *Journal of Physical Chemistry A*, 1998, 102: 173–180.
- [24] TANG I N, FUNG K H, IMRE D G, MUNKELWITZ H R. Phase transformation and metastability of hygroscopic microparticles [J]. *Aerosol Science and Technology*, 1995, 23: 443–453.
- [25] COHEN M D, FLAGAN R C, SEINFELD J H. Studies of concentrated electrolyte solutions using the electrodynamic balance. 1. Water activities for single-electrolyte solutions [J]. *The Journal of Physical Chemistry*, 1987, 91: 4563–4574.
- [26] PROSEK T, LVERSEN A, TAXÉN C, THIERRY D. Low-temperature stress corrosion cracking of stainless steels in the atmosphere in the presence of chloride deposits [J]. *Corrosion*, 2009, 65: 105–117.
- [27] HASTUTY S, NISHIKATA A, TSURU T. Pitting corrosion of Type 430 stainless steel under chloride solution droplet [J]. *Corrosion Science*, 2010, 52: 2035–2043.
- [28] GOU Guo-jing, MA Pei-hua, CHU Min-xiong. Kinetics of synthetic of Cl⁻ type hydrotalcitelike with coprecipitation reaction [J]. *Acta Physico-Chimica Sinica*, 2004, 20: 1357–1363.
- [29] WONG K P, ALKIRE R C. Local chemistry and growth of single corrosion pits in aluminum [J]. *Journal of the Electrochemical Society*, 1990, 137: 3010–3015.
- [30] PARK J O, PAIK C H, HUANG Y H, ALKIRE R C. Influence of Fe-rich intermetallic inclusions on pit initiation on aluminium alloys in aerated NaCl [J]. *Journal of the Electrochemical Society*, 1999, 146: 517–523.
- [31] ALDYKIEWICZ A J, DAVENPORT A J, ISAACS H S. Studies of the formation of cerium-rich protective films using X-ray absorption near-edge spectroscopy and rotating disk electrode methods [J]. *Journal of the Electrochemical Society*, 1996, 143: 147–154.
- [32] SCHNEIDER O, ILEVBARÉ G O, SCULLY J R, KELLY R G. In situ confocal laser scanning microscopy of AA 2024-T3 corrosion metrology: II. Trench formation around particles [J]. *Journal of the Electrochemical Society*, 2004, 151: B465–B472.
- [33] WANG Jun, WANG Zhen-yao, KE Wei. Corrosion behaviour of weathering steel in diluted Qinghai Salt Lake water in a laboratory accelerated test that involved cyclic wet/dry conditions [J]. *Materials Chemistry and Physics*, 2010, 124: 952–958.
- [34] LI Ying. Formation of nano-crystalline corrosion products on Zn–Al alloy coating exposed to seawater [J]. *Corrosion Science*, 2001, 43: 1793–1800.
- [35] VOLOVITCH P, VU T N, ALLÉLY C, AAL A A, OGLE K. Understanding corrosion via corrosion product characterisation: II. Role of alloying elements in improving the corrosion resistance of Zn–Al–Mg coatings on steel [J]. *Corrosion Science*, 2011, 53: 2437–2445.

以 MgCl_2 为主的混合盐对 2024 铝合金大气腐蚀的影响

王彬彬, 王振尧, 韩薇, 汪川, 柯伟

中国科学院金属研究所 金属腐蚀与防护国家重点实验室, 沈阳 110016

摘要: 以盐湖水为腐蚀介质, 通过实验室模拟循环干湿交替实验及电偶电流测量等电化学手段, 利用扫描电镜(SEM)、透射电镜(TEM)、X射线能谱仪(EDS)、电子探针(EPMA)、X射线衍射(XRD)、红外光谱(IR)和大气腐蚀监测仪(ACM)等分析和测量技术, 研究模拟盐湖大气环境下, 可溶性镁盐(主要为 MgCl_2)对 2024 铝合金大气腐蚀行为的影响。结果表明, 在相对湿度低于 30%的环境下, 仍有腐蚀行为发生; 腐蚀产物中出现了含氯的镁铝双金属氢氧化物—— $[\text{Mg}_{1-x}\text{Al}_x(\text{OH})_2]^{x+} \text{Cl}_x^- \cdot m\text{H}_2\text{O}$ (LDH-Cl), 并作为主要腐蚀产物。分析表明, 以 MgCl_2 为主的混合盐不仅在较低的相对湿度下为金属腐蚀的进行提供所需的液膜环境, 同时也作为反应产物参与腐蚀反应。

关键词: 铝合金 2024; 大气腐蚀; 氯化镁; 相对湿度; 腐蚀产物

(Edited by Sai-qian YUAN)